ORIGINAL ARTICLE

Chatter Identification of Face Milling Operation via Time-Frequency and Fourier Analysis

Ching-Chih Wei[1], Meng-Kun Liu[1,*], and Guo-Hua Huang[1]

[1] *Department of Mechanical Engineering, National Taiwan University of Science and Technology, 106 Taipei city, TAIWAN*

(**Received** 30 September 2015; **Accepted** 8 January 2016; **Published on line** 1 March 2016)

*Corresponding author: mkliu@mail.ntust.edu.tw

DOI: 10.5875/ausmt.v6i1.1018

Abstract: Chatter is generally defined as self-generated vibrations from the interaction between tool and workpiece. It is the most critical vibration in machining operations and can decrease the surface quality and cause the premature tool wear. Chatter creates erroneous vibrations on the workpiece surface. However, even though the spatial response of chatter is still bounded, its frequency response would become unstably broadband, emitting high-pitched sounds. The deterioration in both time and frequency domains implies that chatter is a route-to-chaos process. To capture the time-frequency characteristics of chatter, instantaneous frequency is applied to extract the relevant force vibration of machining chatter, and the energy ratio approach is used to develop a discrete stability lobe diagram of a face-milling operation. The proposed method is validated by measuring the surface roughness of the workpiece.

Keywords: chatter, milling, Hilbert-Huang transform, Fourier transform, stability lobe diagram

Introduction

Machining operations result in many kinds of vibrations from the machine, tool or workpiece. The most critical such vibration is vibration generated from interaction between the tool and the workpiece. This so-called “chatter” results in tool wear and reduces workpiece surface quality. Operators usually seek to alleviate chatter by reducing cutting parameters such as feed rate, spindle speed and depth of cut (DOC), but such measures also decrease the material removal rate (MRR) and thus overall throughput. To increase both cutting efficiency and fabrication quality, it is imperative to establish the relation between various cutting parameters and the incidence of chatter. Currently, the stability lobe diagram is widely used to identify a stable cutting region in turning and milling operations. In the late 1950s, Tobias and Fishwick [1] explained the regeneration mechanism and developed the two-dimensional stability lobe theory, which relates the cutting stability to the function of spindle speed and DOC. The stability lobe diagram has been widely applied in numerical methods. Generally, machine tool dynamics are identified through impact testing and is represented in the frequency response function (FRF). With this information, the stability lobe diagram could predict cutting conditions through a mechanistic force model of the milling process. As shown in Fig. 1, the stable cutting region is defined by the spindle speed and DOC. Chatter occurs when the cutting parameters are chosen above the curves, otherwise the cutting process is stable. The establishment of a stability lobe diagram assumes that the tool vibration can be approximated by a second order linear differential equation, where the FRF is used to determine the marginal DOC. The stable cutting region is seen as a “good” alignment (i.e., in phase) between the tool and the workpiece vibration, while the unstable cutting region means the vibrations are out of phase [2]. By drawing the stability lobe diagram in advance, the operator could easily choose and design the optimal cutting parameters to maximize cutting efficiency. To validate the cutting stability margin in the machining operation, Fast Fourier Transform (FFT) is usually used to analyze the vibration signal [3][4]. Once chatter occurs, excessively high frequencies would appear on the frequency spectrum.

However, previous studies have indicated that the regenerative cutting process contains rich nonlinear

characteristics, and the linear approximation used in the stability lobe diagram would inevitably misinterpret the genuine features of nonlinear vibration [5]. Machining chatter is a route-to-chaos process with deterioration in both the time and frequency domains. Despite the time response of the vibration being bounded, when chatter occurs the frequency response would become unstably broadband. Hence, to capture the bona fide features of the machining status, it is necessary to monitor time and frequency response simultaneously.

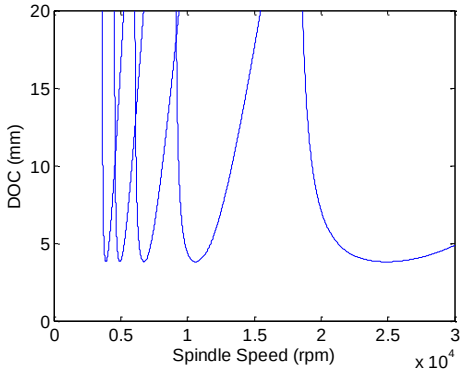

Figure 1. Stability lobe diagram.

Recently, instantaneous frequency (IF) using the Hilbert-Huang transform (HHT) has been used to investigate machining vibration. Ensemble empirical mode decomposition (EEMD) applies the shifting process to decompose the nonlinear broadband response into orthogonal sets of mono-component called intrinsic mode function (IMF). EEMD can separate a complex time series into simple oscillatory modes [6][7]. The Hilbert transform is then applied to each IMF and resolves the instantaneous frequency, giving both time and frequency resolution concurrently. EEMD has been used to decompose vibration signals into multiple IMFs; FFT was then applied to compare the frequency of stable and unstable cutting to identify the chatter frequency [8]. HHT was applied directly to obtain a time-frequency diagram of the vibration signal, and the marginal spectrum was used to observe the frequency distribution [9]. In general, previous studies measured the cutting force along the X and Y direction of an end-milling process, which is the main cause of tool vibration. A two-direction force sensor is required to measure the cutting force.

This research seeks to measure the signal of the cutting force in the Z (vertical) direction in a face-milling operation to analyze the signal and identify chatter. To capture the genuine characteristics of the machining status, EEMD is applied to decompose the force signal into multiple IMFs. Those related to the machining process will be extracted and combined, while the irrelevant IMFs will be ignored. Hence the EEMD process serves as an empirical filter to evaluate machining vibration and discard environmental noise. FFT will be used to analyze the combined IMFs and a method to calculate energy ratio will be proposed to determine the occurrence of chatter. Finally, a discrete stability lobe diagram is drawn and validated according to the surface roughness of the workpiece.

Experimental Design and Setup

Figure 2(a) shows a 3-axis milling machine used for the cutting experiment, with its specification summarized in Table 1. This cutting machine differs from a CNC machine center in two key respects. First, because the torque of its spindle is limited, it only removes a small amount of chip each time so that a high spindle speed is required to increase cutting capability. Second, this machine is designed to provide a low DOC and a high feed rate during high speed cutting (HSC), so it has low stiffness and small inertia. The cutting experiment uses a 6 mm end-mill tool as shown in Fig. 2(b), and the cutting force during face milling is measured using a Kistler 6-axis dynamometer as shown in Fig. 2(c), with the specification summarized in Table 2. The sampling rate in the experiment is 10000 Hz, which is 50 times of the maximum frequency at 12000 rpm. The signal is then analyzed using HHT and FFT. After the signal of the cutting force in the Z direction (vertical) is analyzed, the results are compared against the surface roughness, which is measured by surface metrology equipment as shown in Fig. 2(d), and the relation among cutting parameters, cutting force and the surface quality can be established.

Ching-Chih Wei received his B.Eng. and M.Eng. Degrees in Mechanical engineering from National Taiwan University of Science and Technology, in 2012 and 2014 respectively. He has worked in Precision 5-axis CNC Machining Center in National Taiwan University of Science and Technology for 2 years. His work includes conducting CNC training programs and managing CNC machines. He enrolled the Ph.D. program in National Taiwan University of Science and Technology in 2014. His current research is mainly about 5-axis machine and machining technique, including Kinematics, Cutting optimization, Signal analysis, Computer programming, Mechanical design and Mechatronics.

Meng-Kun Liu received his bachelor degree from National Chiao Tung University and master degree from National Taiwan University, both in mechanical engineering. He obtained his PhD in Mechanical Engineering from Texas A&M University in 2012. Since 2015, He joined the department of Mechanical Engineering in National Taiwan University of Science and Technology as an assistant professor. Dr. Liu's research interests include time-frequency analysis of manufacturing process, sensorless fault diagnosis of induction motors, robot force control and chaos control. He has co-authored numerous journal articles, conference proceedings and a book published by Wiley.

Guo-Hua Huang was graduated from National Taiwan University of Science and Technology and enrolled the M.Eng. Program in the same college in 2014. His electives are mainly regarding the signal processing and the structural design. In addition, he has done the mechanical test of materials in Lab for one years. He is currently researching into the application of the multi-axis rapid prototyping machine about using multiple materials for combine.

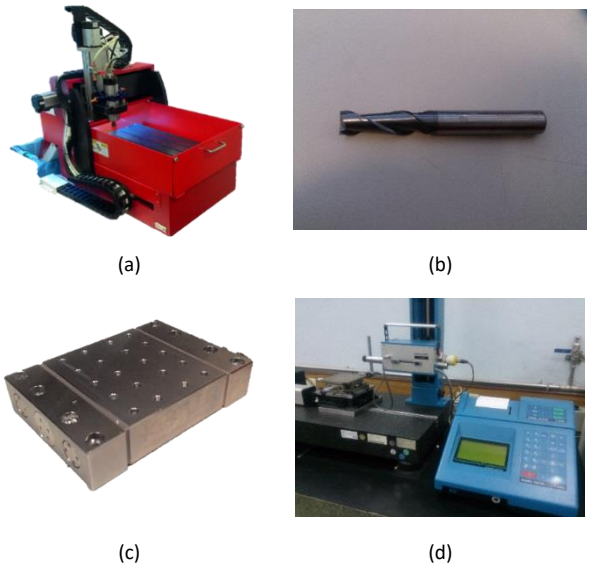

(a) (b) (c) (d)

Figure 2. Experimental equipment: (a) CNC milling machine; (b) 6 mm end-mill tool; (c) 6-axis dynamometer; (d) Surface metrology equipment.

CNC milling machine	
Travels X / Y / Z	300 / 350 / 150 mm
Max. feed rate	10 m / min
Max. spindle speed	12000 rpm
Repeatability	0.01 mm

Table 1. Specification of CNC milling machine.

6-axis dynamometer		
Measuring range	Fx, Fy, Fz	±10 kN
	Mx, My, Mz	±500 Nm
Maximum sampling rate	125kS / s	

Table 2. Specification of 6-axis dynamometer.

As previously mentioned, the three important cutting parameters are feed rate, spindle speed and DOC. The experiment is divided into two categories, one sets the feed rate as a constant, and investigates the relation between spindle speed and DOC; the other sets the DOC as a constant, and investigates the relation between spindle speed and feed rate. Meanwhile, the DOC can be classified as the axial depth of cut (ap) and radial depth of cut (ae). In both experiments, the radial depth of cut is set as 50% of the tool radius, which is 3 mm, and the DOC in this research always refers to the axial depth of cut.

The first experiment uses a ladder-shaped workpiece (shown in Fig. 3) and a base fixture is designed to be fixed on the 6-axis dynamometer. The recommended cutting parameters are summarized in Table 3. With the recommended MRR, the critical DOC is about 0.24 mm, which is calculated from Eq. (1). However, the DOC of 0.24 mm is not efficient for rough milling, thus to determine optimal cutting efficiency and quality, the DOC is designed from 2 mm to 12 mm with an interval of 2 mm in each step. Using the recommended cutting parameters and cutting capability, the spindle speed is set from 6000 rpm to 12000 rpm with an interval of 1000 rpm. Because the tool is a 2-flute end-mill and the feed per tooth is set as 0.01 mm/tooth, the feed rate can be calculated by Eq. (2). The second experiment uses a flat workpiece and the DOC is fixed at 2 mm. The feed rate is changed from 400 mm/min to 1000 mm/min with an interval of 200 mm/min, and the adjustment of spindle speed is the same as in the first experiment.

$$MRR = a_p \cdot a_e \cdot F \quad (1)$$

MRR: Material Removal Rate

a_p: Axial depth of cut

a_e: Radial depth of cut

F: Feed rate

$$F = f_z \cdot z \cdot N \quad (2)$$

F: Feed rate

f: Feed per tooth

z: Number of flutes

N: Spindle speed

6 mm end-mill tool (aluminum workpiece)	
Spindle speed	7900 rpm
Feed rate	424 mm/min
Material Removal Rate	305.28 mm^3/min

Table 3. Cutting parameters recommendation.

Figure 3. Designed ladder workpiece and fixture.

Methods of Signal Analysis

This research investigates chatter in a face milling operation from a time-frequency perspective. The force in the vertical direction is measured and analyzed as shown in Fig. 4, and Fig. 5 presents the analysis flow. Both experiments begin by measuring the force signal in the vertical direction. EEMD is used to decompose the original signal into multiple independent IMFs. Then instantaneous frequency (IF) is calculated from each IMF using the Hilbert transform. With the IF result, the

dominant IMFs which best represent the occurrence of chatter can be selected and combined to form a delegated signal. Next, the dominant frequencies of this delegated signal can be found by using Fast Fourier Transform (FFT), and chatter can be identified by observing the energy change of the dominant frequencies. Finally, the surface roughness of the workpiece is measured to validate the result and construct the discrete stability lobe diagram.

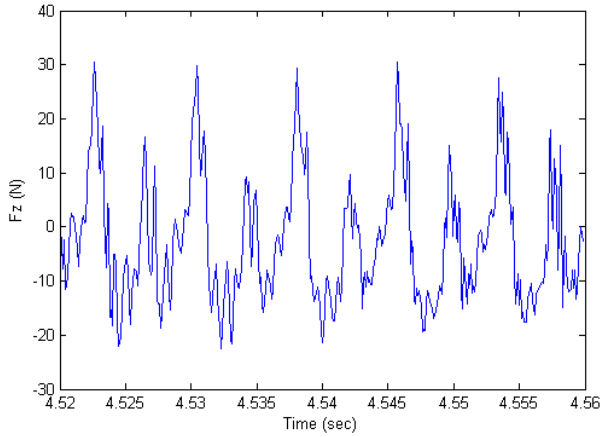

Figure 4. Measured force signal in z-axis.

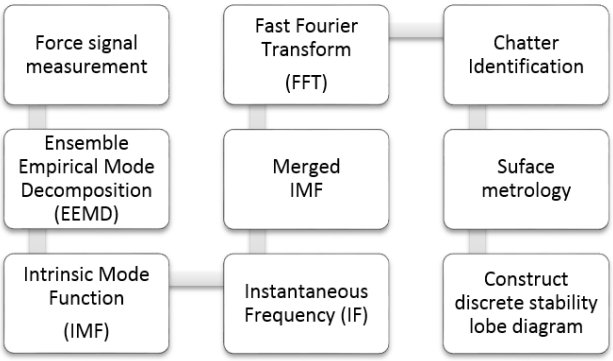

Figure 5. Flow chart of the methods.

Methods of Signal Analysis

Instantaneous frequency has been previously used to investigate the nonlinear features of a time-delayed feedback oscillator, along with phase plots, bifurcation diagrams, and Fourier spectrum [10]. Ensemble empirical mode decomposition (EEMD) applies the shifting process to decompose the nonlinear broadband response into orthogonal set of mono-components called intrinsic mod function (IMF). EEMD can separate a complex time series into simple oscillatory modes. Each IMF has the same number of extrema and zero crossings so that it is inherently symmetrical with respect to the local mean defined by the average of the upper and lower cubic spline envelope without resorting to any pre-defined basis. EEMD is needed to deal with data from nonstationary and nonlinear processes. The EEMD process is shown in Fig. 6 and is elucidated in [7].

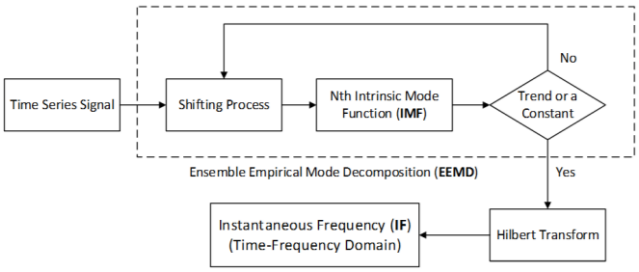

Figure 6. Process of Hilbert-Huang Transform (HHT).

A decomposition of the original time series signal into n IMFs can be represented as:

$$x(t)=\sum_{j=1}^{n}C_j(t)+R(t) \tag{3}$$

where C_j (t) is the jth intrinsic mode function and the residue R(t) can be either the mean trend or a constant. Equation (3) also indicates that the original signal can be synthesized by IMFs and residue, so the completeness of this decomposition can be proofed numerically. The ratio of each IMF energy compared to the total energy can be calculated as:

$$r_j=\frac{\int_0^T\left|C_j(t)\right|^2dt}{\int_0^T\left|x(t)\right|^2dt} \tag{4}$$

The energy ratio of each IMF can be used to determine the dominate dominant frequency component within the input signal x(t). To resolve the instantaneous frequency, the Hilbert transform is applied to each IMF and constructs an analytic signal Z_j (t).

$$\begin{aligned}Z_j(t)&=C_j(t)+iH\left[C_j(t)\right]\\&=C_j(t)+iy_j(t)\\&=a_j(t)e^{i(\phi_j(t))}\end{aligned} \tag{5}$$

where the Hilbert transform is:

$$y_j(t)=H\left[C_j(t)\right]=\frac{P}{\pi}\int_{-\infty}^{\infty}\frac{C_j(\tau)}{t-\tau}d\tau \tag{6}$$

P is the Cauchy principle value. Then $a_j(t)=\sqrt{C_j^2(t)+y_j^2(t)}$ and the instantaneous frequency of the jth IMF can be defined as:

$$f_j=\frac{1}{2\pi}\frac{d\phi_j(t)}{dt} \tag{7}$$

Thus the frequency modulation of a complex signal can be retrieved. The integral of the Hilbert spectrum throughout the entire time span can be defined as a marginal spectrum as follows [6]:

$$h(\omega)=\int_0^T H(\omega,t)dt \tag{8}$$

The marginal spectrum offers a measure of the total energy contribution from each frequency value. It represents the accumulated energy distribution over the entire data span in a probabilistic sense.

Results and Discussion

Experiment I: Constant feed rate

First, the cutting force signal is decomposed into multiple IMFs using EEMD, as shown in Fig. 7. Then each IMF is converted to an instantaneous frequency using the Hilbert transform, as shown in Fig. 8. It is shown that, even in stable cutting conditions, the measured vertical force contains rich nonlinear dynamics. The instantaneous frequency of each IMF in Fig. 8 is not constant, but rather shows intermittent variations, a characteristic of the regenerative effect. To observe each instantaneous frequency from a probability perspective, they are transformed to a marginal spectrum, as shown in Fig. 9, which shows the bandwidth of each IMF under different DOCs. The spindle speed in this experiment ranges from 6000 rpm to 12000 rpm, with corresponding spindle frequencies of 100 Hz to 200 Hz. Given that harmonics may be as much as four times the spindle frequency, we observed frequencies between 100Hz and 1000Hz. Figure 8 shows temporal intermittent variations and represents the real frequency in each IMF, thus we can retain IMF4, IMF5, and IMF6 and omit the irrelevant IMFs.

When the spindle speed is set to 6000 rpm, the instantaneous frequencies of IMF4, IMF5 and IMF6 are transformed into a marginal spectrum as shown in Fig. 9. With the DOC increment, the bandwidth of each marginal spectrum becomes broader and the spectrum peak, i.e., the frequency with the highest probability of occurring, shifts to the right, meaning a higher overall frequency. Take IMF 6 in Fig. 9 for example: When the DOC increases, the peak frequency is still obvious but it shifts from 100Hz to 150Hz and the bandwidth widens. When the spindle speed is set to 12000 rpm, the change of marginal spectrum has the same tendency as the spindle speed at 6000 rpm. As shown in Fig. 10, the dominant frequency at 200 Hz is also obvious in IMF6 when the DOC is 2mm, but the bandwidth is wider with the larger DOC. As a result, the marginal spectrum of the specific IMFs can reflect subtle changes to the machining status.

To design a quantifiable index to identify machining chatter, the signals of IMF4, IMF5, and IMF6 are combined and FFT is applied to extract the dominate frequencies, as shown in Fig. 11. The frequency of 200 Hz is found to be the dominant frequency caused by spindle speed, 400 Hz is the tool natural frequency in two-flute cutting, and 600 Hz and 800 Hz are respectively the three-time and four-time frequencies caused by the spindle vibration. The excessive frequencies on the Fourier spectrum increase with the DOC. Moreover, based on experimental observations, the force signal which has a broadband distribution in frequency can be identified as the occurrence of chatter, as shown in Fig. 11(c).

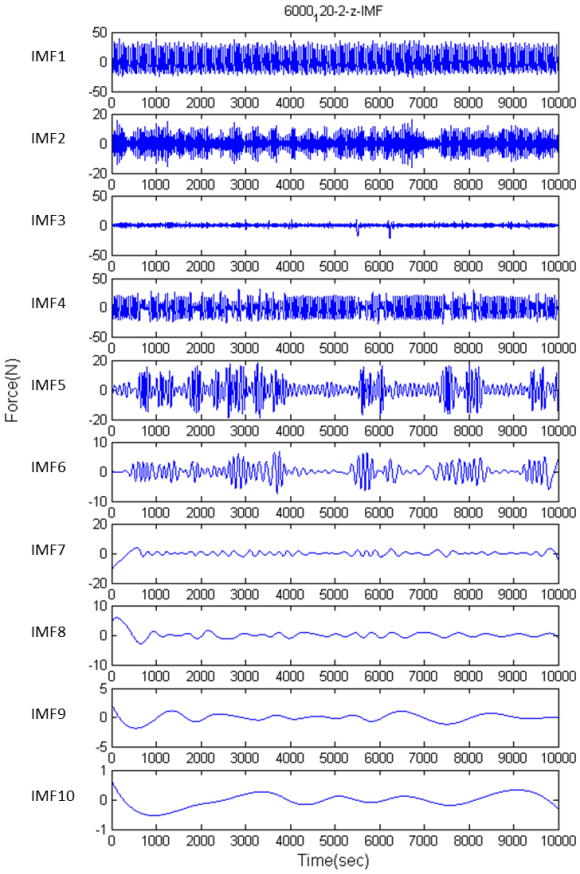

Figure 7. IMF signal (spindle speed is 6000 rpm and DOC is 2 mm).

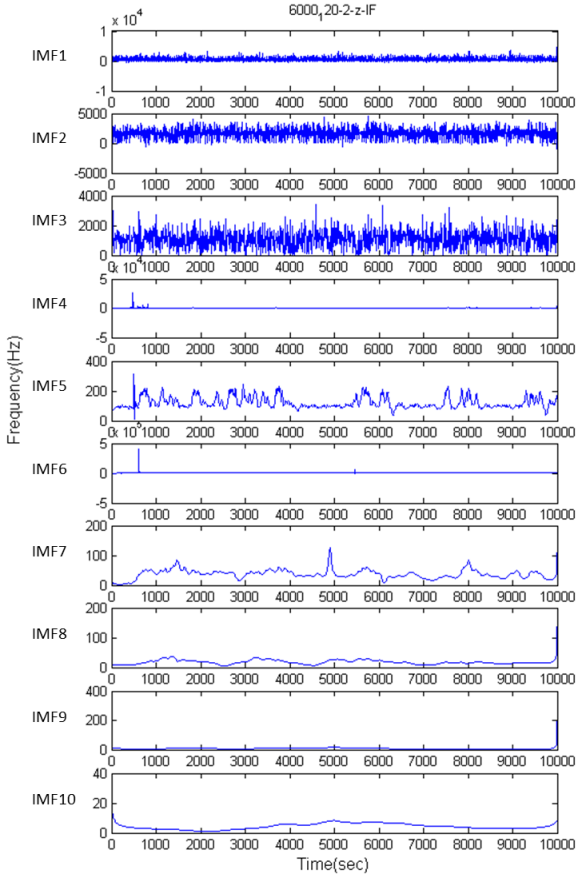

Figure 8. Instantaneous frequency of each IMF (spindle speed is 6000 rpm and DOC is 2 mm).

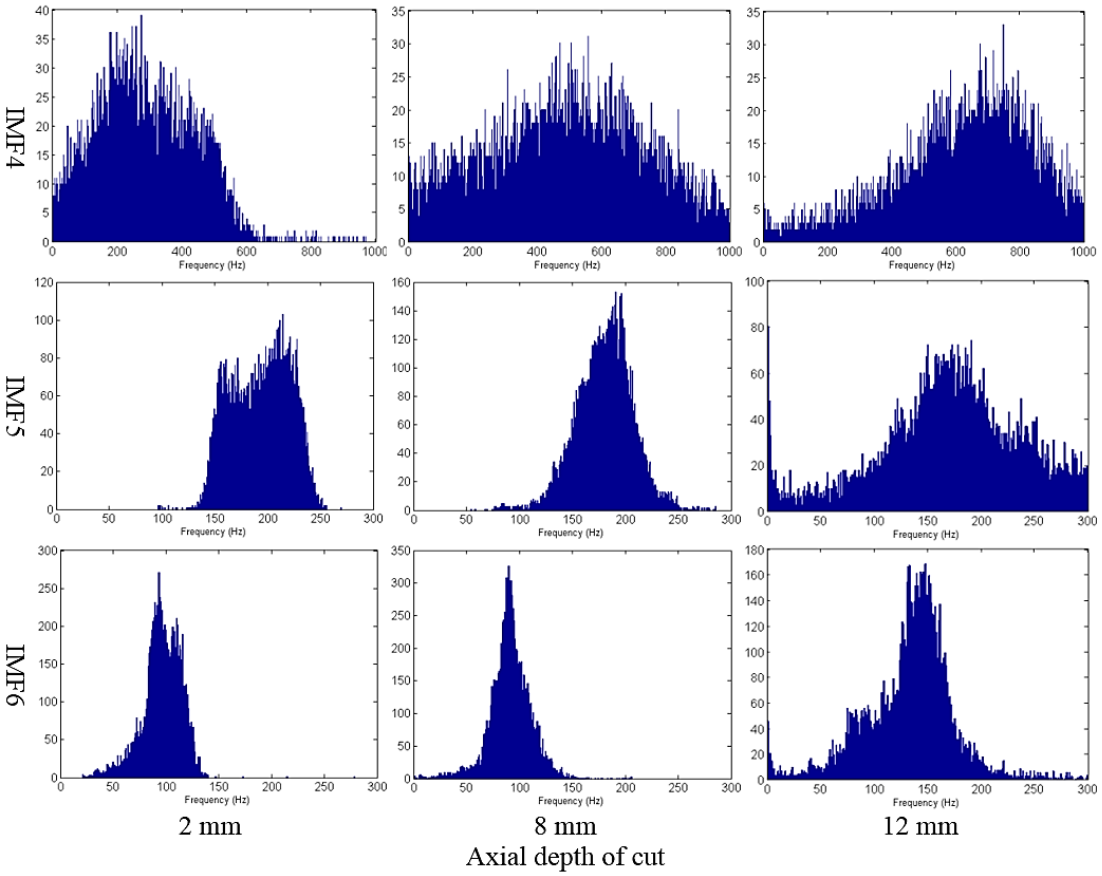

Figure 9. Marginal spectrum (spindle speed is 6000 rpm).

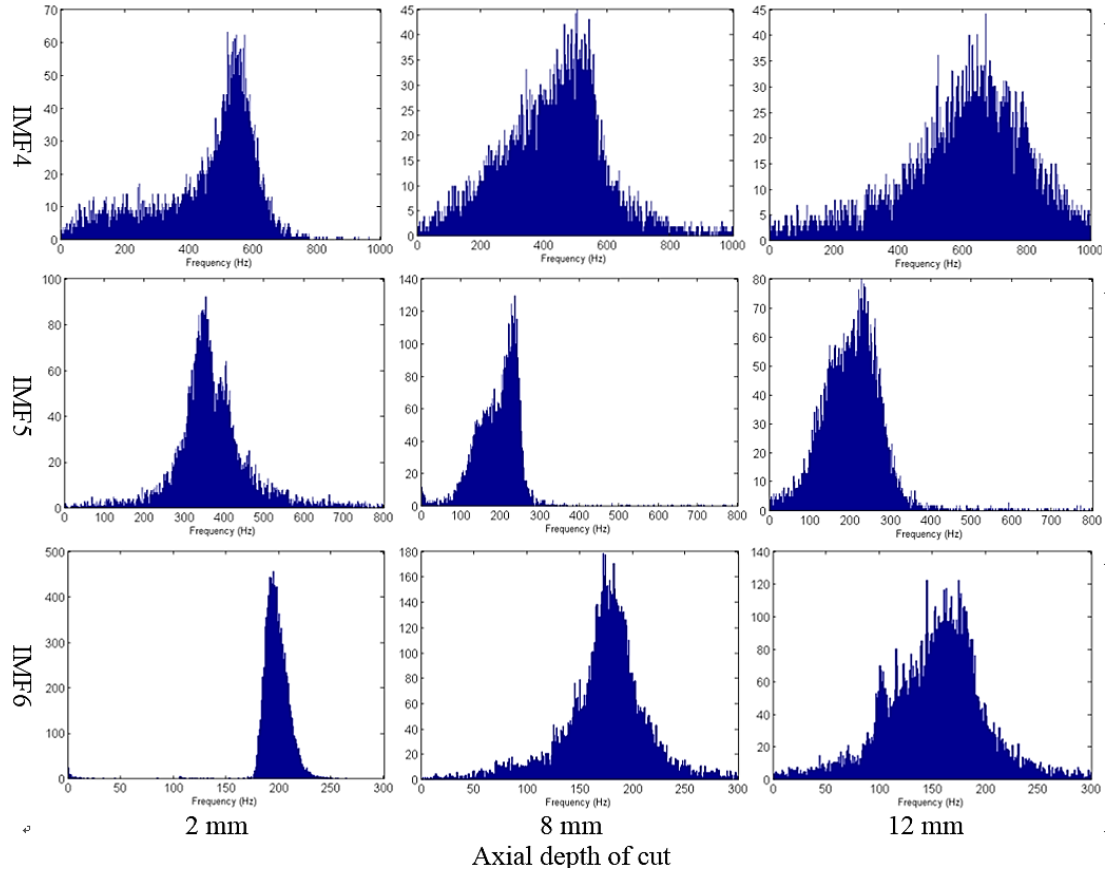

Figure 10. Marginal spectrum (spindle speed is 12000 rpm).

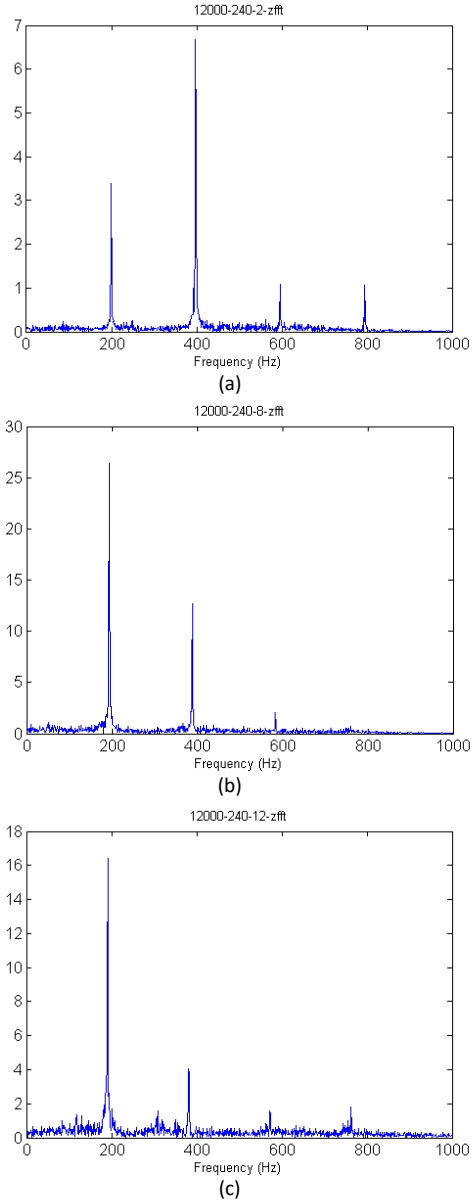

Figure 11. FFT of merged IMF (spindle speed is 12000 rpm) (a) DOC is 2mm; (b) DOC is 8 mm; (c) DOC is 12 mm.

Although chatter can be observed from Fig. 11(c), chatter must still be determined quantitatively. The FFT results of the combined IMF show the magnitude of the main cutting frequencies is much higher than the others, which means the frequencies of the main cutting signals dominate the rest of the vibration signal. Figure 11 shows the energy ratio between two dominant frequencies (spindle frequency and tool dominant frequency) and the combined signal can be designed as:

$$Energy \quad ratio = \frac{(A+B)}{\sum_{f=0}^{f=1000} P(f)} \tag{9}$$

where

A: Magnitude of spindle frequency

B: Magnitude of tool natural frequency

P(f): Magnitude of frequency f

A, B, and P(f) are measured based on the Fourier spectrum of the combined signal of IMF4, IMF5 and IMF6 in Fig. 11, which refers to frequencies below 1000 Hz, so the frequency in the Fourier spectrum is chosen in the same range. The design of the energy ratio in Eq. (9) is based on the assumption that chatter will produce excessive frequencies, and the energy generated will dilute the ratio of the dominant frequencies' energy with respect to the overall energy. Therefore a threshold can be set to determine the drop in the energy ratio, indicating the occurrence of chatter. To validate this assumption, the surface roughness of the workpiece is measured to compare the energy ratio to the surface quality. As a result, the discrete stability lobe diagram is constructed based on the proposed criteria. Because there the FFT results may include noise, a threshold value is set to filter low-effect frequencies whose energy is less than 1/20 of the energy from the dominant frequency generated by the spindle speed. After filtering the signal, the energy ratio of the dominant frequencies under different cutting parameters is developed, as shown in Table 4. Holding spindle speed constant, the ratio decreases as the DOC increases. The surface roughness of the workpiece is then measured and the results are shown in Table 5. From Tables 4 and 5, the energy ratio and surface roughness can be presented together in Fig. 12. It can be seen that the energy ratio above 0.25 has a better surface roughness within 1 μm. By setting the energy ratio 0.25 as the margin of chatter occurrence, the discrete stability lobe diagram can be constructed, as shown in Fig. 13. Figure 14 shows the workpiece surface after cutting, which can be classified as stable and unstable regions according to surface roughness, and those regions are completely consistent with the results of the discrete stability lobe diagram.

Experiment II: Constant DOC

The signal analysis process in experiment II is the same that in experiment I. First, the cutting force signal is decomposed into multiple IMFs using EEMD, and then each IMF is converted into a marginal spectrum. In Fig. 15, the dominant frequency of IMF6 is about 133 Hz, which is created by a spindle speed of 8000 rpm. The bandwidth in each IMF exhibits no obvious difference, and the peak frequency remains the same, meaning that the change in machining status is opaque. Likewise, the dominant frequency of IMF6 in Fig. 16 is about 200Hz, due to the spindle speed of 12000 rpm. Among four different feed rate conditions, the dominant frequency is much clearer when the feed rate in 400 mm/min, indicating that this rate produces a small nonlinear vibration effect and possibly the best surface quality. The marginal spectrum in other three conditions shows no obvious difference, which implies similar cutting conditions.

For further discussion, the signals of IMF4, IMF5 and IMF6 are combined and processed using FFT analysis. The FFT result for a spindle speed of 12000 rpm is shown in Fig. 17. As in the FFT analysis in experiment I, the dominant frequency and tool natural frequency are easily identified. As the feed rate increases, the abnormal vibration becomes more prominent, especially at a feed rate of 800 mm/min.

Figure 18 shows the workpiece surface after cutting. The region is divided into stable and unstable cutting according to the feed rate and spindle speed. The energy ratio is then constructed in Table 6 and the surface roughness is recorded in Table 7. The relation between the energy ratio and the surface roughness is drawn in Fig. 19. However, the machine in this research has low stiffness and may vibrate easily. Even though the energy ratio is less than 0.1, the surface roughness is around 1 µm which is still acceptable. Hence the stability margin for experiment II is opaque. But for most results, the tendency is that, as the energy ratio increases, the surface roughness converges to the better region that is mostly less than 1 µm.

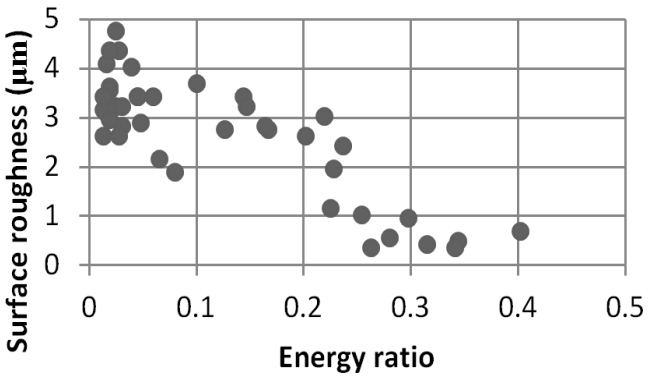

Figure 12. Relation of energy ratio and surface roughness.

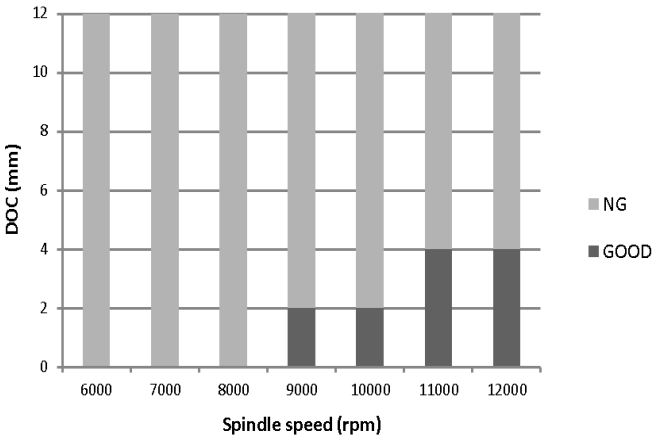

Figure 13 Discrete stability lobe diagram.

Energy Ratio		Spindle speed (rpm)						
		6000	7000	8000	9000	10000	11000	12000
DOC (mm)	12	0.016	0.018	0.021	0.015	0.015	0.026	0.031
	10	0.020	0.028	0.019	0.023	0.023	0.061	0.043
	8	0.030	0.032	0.052	0.034	0.049	0.148	0.103
	6	0.022	0.049	0.130	0.147	0.203	0.227	0.168
	4	0.068	0.222	0.171	0.239	0.230	0.301	0.283
	2	0.083	0.256	0.404	0.317	0.346	0.265	0.345

Gray area: energy ration greater than 0.25 (stable cutting region)

Table 4. Energy ratio of dominant frequency to other frequencies.

Roughness (µm)		Spindle speed (rpm)						
		6000	7000	8000	9000	10000	11000	12000
DOC (mm)	12	3.07	3.05	3.53	3.37	2.60	4.70	2.56
	10	4.01	3.17	3.34	4.28	2.92	3.37	3.97
	8	4.33	3.17	2.84	2.74	3.35	3.20	3.66
	6	3.56	3.38	2.71	3.34	2.57	1.11	2.79
	4	2.10	2.97	2.72	2.37	1.91	0.88	0.48
	2	1.85	0.98	0.61	0.36	0.43	0.33	0.29

Gray area: surface roughness smaller than 1µm (stable cutting region)

Table 5. Surface roughness results.

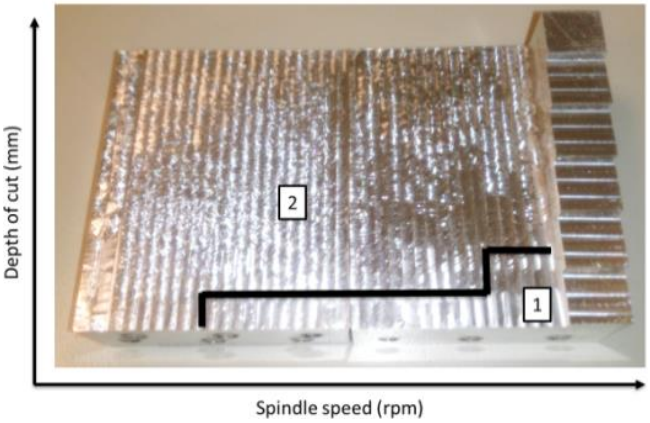

Figure 14. Milling result of experiment I, (1) stable cutting region, (2) unstable cutting region.

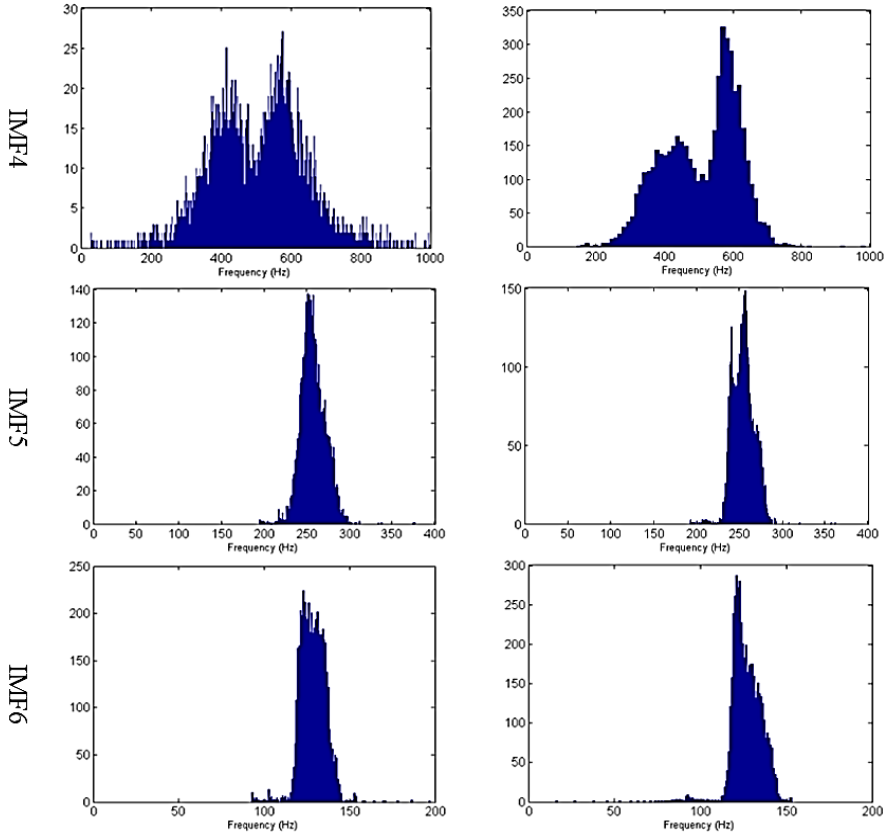

Figure 15. Marginal spectrum with spindle speed at 8000 rpm.

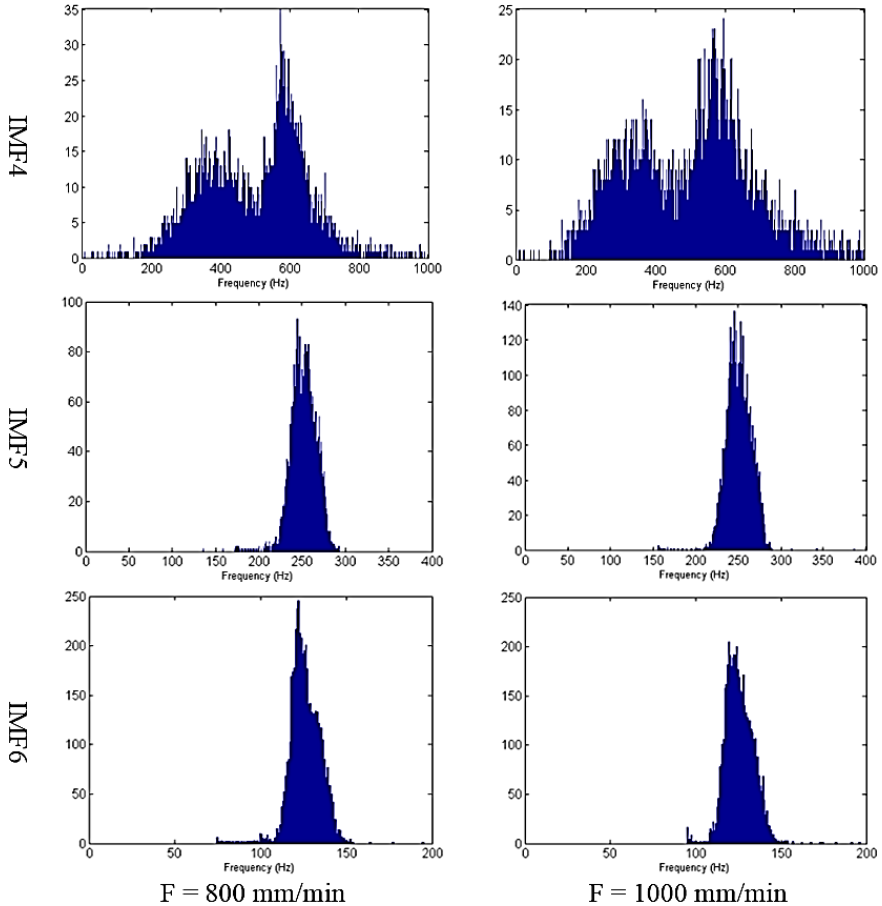

Figure 15. (cont.) Marginal spectrum with spindle speed at 8000 rpm.

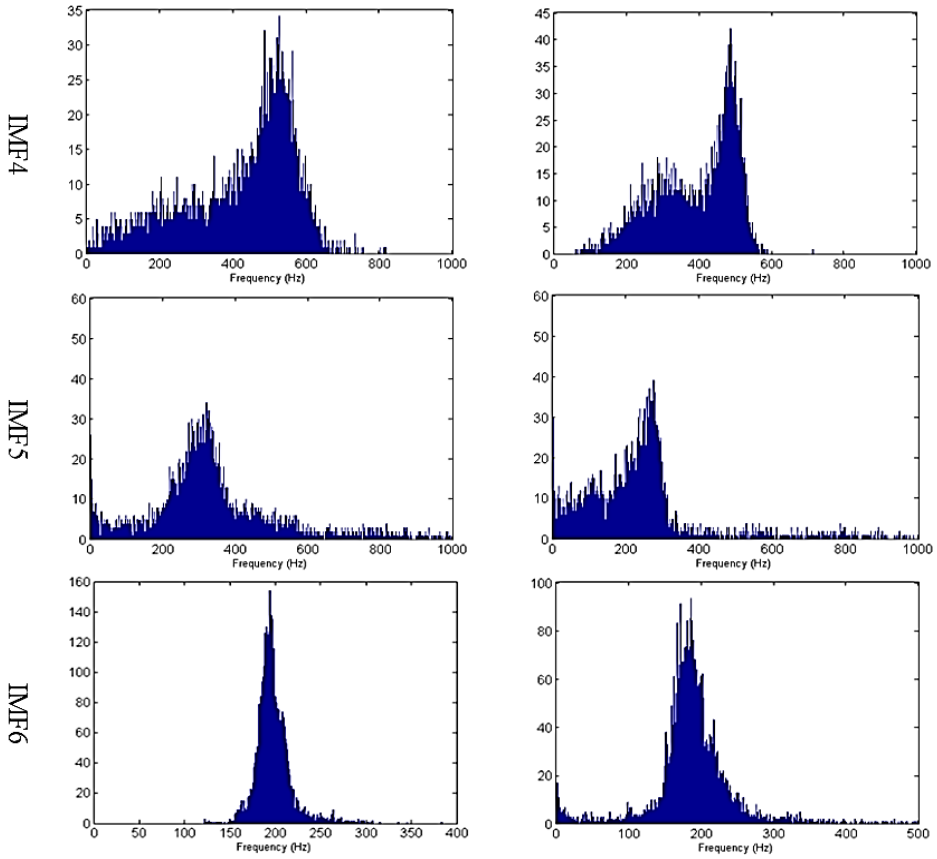

Figure 16. Marginal spectrum with spindle speed at 12000 rpm.

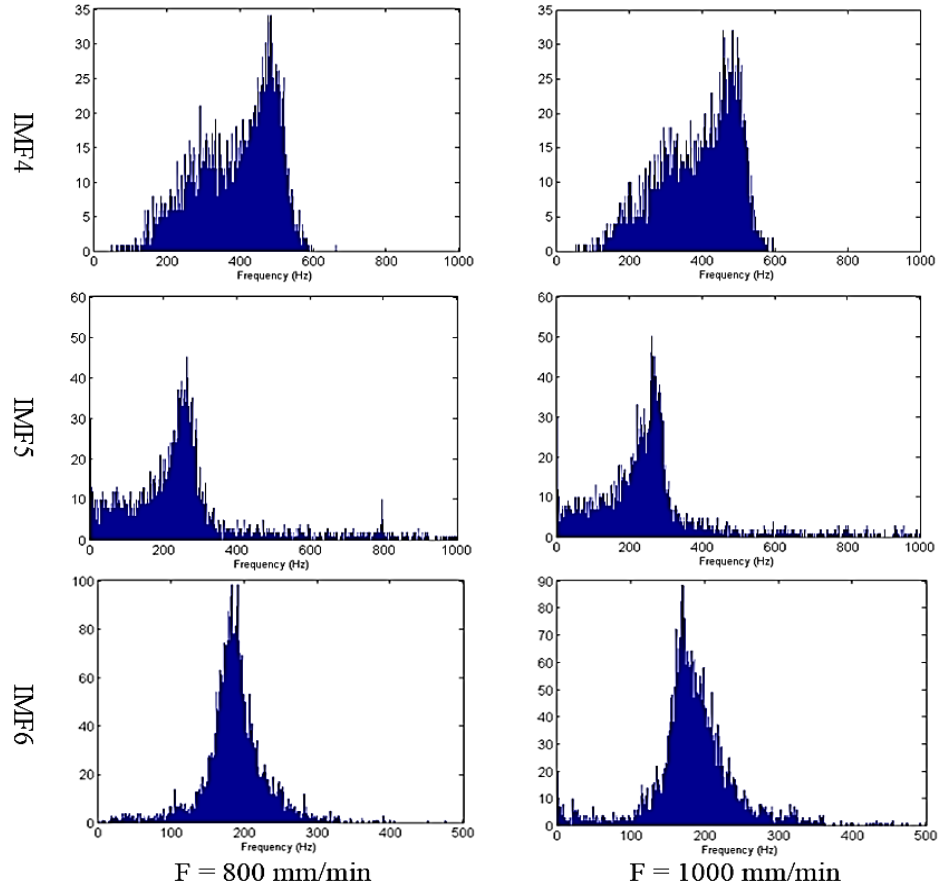

Figure 16. (cont.) Marginal spectrum with spindle speed at 12000 rpm.

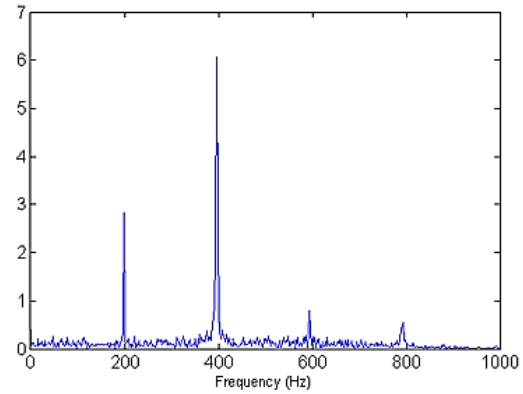

(a)

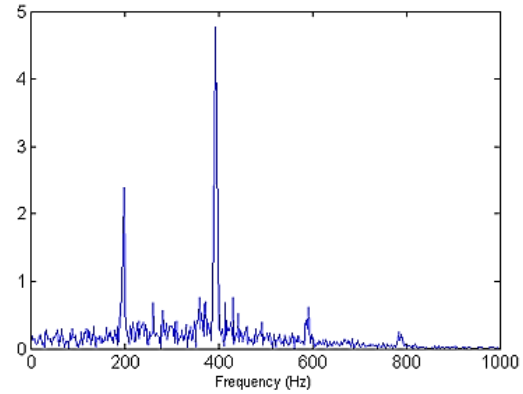

(b)

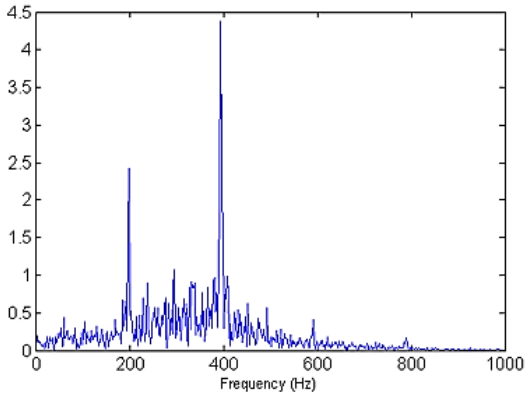

(c)

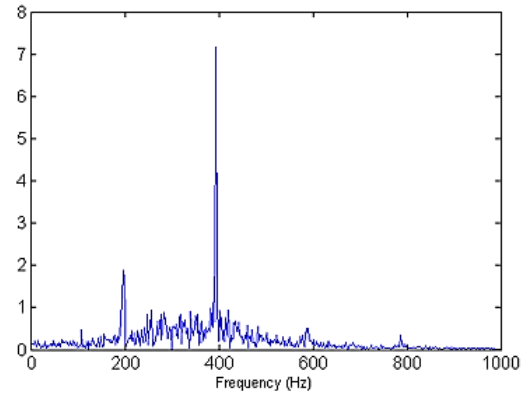

(d)

Figure 17. FFT of combined IMF with spindle speed is at 12000 rpm, (a) Feed rate is 400 mm/min; (b) Feed rate is 600 mm/min; (c) Feed rate is 800 mm/min; (d) Feed rate is 1000 mm/min.

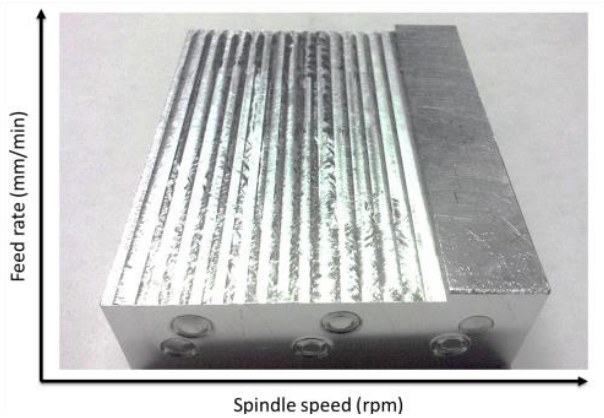

Figure 18. Milling result of experiment II.

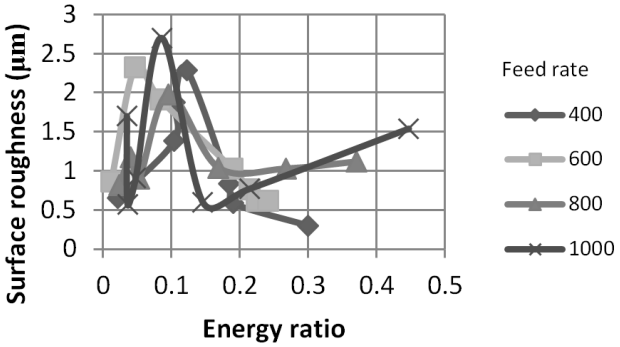

Figure 19. Relation of energy ratio and surface roughness.

Energy ratio		Spindle speed (rpm)						
		6000	7000	8000	9000	10000	11000	12000
Feed rate (mm/min)	1000	0.048	0.036	0.086	0.035	0.447	0.214	0.146
	800	0.041	0.053	0.096	0.024	0.371	0.267	0.169
	600	0.084	0.047	0.189	0.012	0.214	0.241	0.225
	400	0.104	0.105	0.123	0.184	0.022	0.190	0.300

Table 6. Energy ratio of dominant frequency to other frequencies.

Roughness (μm)		Spindle speed (rpm)						
		6000	7000	8000	9000	10000	11000	12000
Feed rate (mm/min)	1000	0.91	0.57	2.70	1.70	1.54	0.77	0.6
	800	1.17	0.9	1.98	0.82	1.12	1.03	1.04
	600	1.91	2.32	1.03	0.86	0.76	0.46	0.62
	400	1.38	1.88	2.29	0.84	0.65	0.59	0.30

Table 7. Surface roughness results.

Conclusion

A generic chatter identification approach is proposed in this research. To capture the genuine time-

frequency characteristics of chatter, the Hilbert-Huang transform is used as an empirical filter to extract the relevant machining force signal from a face-milling machine. Different from previous studies, only the vertical force is measured for analysis. The occurrence of chatter is identified by the energy ratio of the dominant frequencies on the FFT spectrum. As a result, a discrete stability lobe diagram is developed by setting a threshold for the energy ratio, and the surface roughness of the workpiece is measured to validate this approach. The results suggest the surface roughness converges to a better quality within 1 μm as the energy ratio is increased. Therefore, the energy ratio proposed in this research can be used as a reference to identify superior cutting conditions.

References

[1] S. A. Tobias and W. Fishwick, "Theory of regenerative machine tool chatter," *The Engineer*, vol. 205, pp. 199-203, 1958.

[2] T. L. Schmitz and K. Scott Smith, *Machining Dynamics: Frequency Response to Improved Productivity*. Springer Science & Business Media, 2008.

[3] Y. Altintas, G. Stepan, D. Merdol, and Z. Dombovari, "Chatter stability of milling in frequency and discrete time domain," *CIRP Journal of Manufacturing Science and Technology*, vol. 1, pp. 35-44, 2008.
doi: 10.1016/j.cirpj.2008.06.003

[4] S. D. Merdol and Y. Altintas, "Multi frequency solution of chatter stability for low immersion milling," *Journal of Manufacturing Science and Engineering* Transactions of the ASME, vol. 126, pp. 459-466, 2004.
doi: 10.1115/1.1765139

[5] C. Steve Suh and M.-K. Liu, *Control of Cutting Vibration and Machining Instability: A Time-Frequency Approach for Precision, Micro and Nano Machining*. John Wiley & Sons, 2013.

[6] N.-E. Huang, Z. Shen, S.-R. Long, M.-C. Wu, H.-H. Shih, Q. Zheng, N.-C. Yen, C.-C. Tung, H.-H. Liu, "The empirical mode decomposition and the Hilbert spectrum for nonlinear and non-stationary time series analysis," *Proceedings of the Royal Society of London A: Mathematical, Physical and Engineering Sciences*, vol. 454, no. 1971, pp. 903–995, 1998.
doi: 10.1098/rspa.1998.0193

[7] N.-E. Huang and S.-S. Shen. *Hilbert-Huang transform and its applications.* World Scientific, 2005.

[8] H. Cao, K. Zhou, and X. Chen, "Chatter identification in end milling process based on EEMD and nonlinear dimensionless indicators," *International Journal of Machine Tools and Manufacture*, vol. 92, pp. 52-59, 2015.
doi: 10.1016/j.ijmachtools.2015.03.002

[9] W. Peng, Z. Hu, L. Yuan, and P. Zhu, "Chatter identification using HHT for boring process," in Proceedings of *SPIE - The International Society for Optical Engineering*, Beijing, China, 2013, p.904316.
doi: 10.1117/12.2037988

[10] C.-S. Suh and B. Yang, "On the nonlinear features of time-delayed feedback oscillators," *Communications in Nonlinear Science and Numerical Simulation*, Vol. 9, No. 5, pp. 515-529, 2004.
doi: 10.1016/S1007-5704(03)00008-X